

Polarization-entangled Bell states generation based on birefringence in high nonlinear microstructure fiber at $1.5 \mu\text{m}$

Qiang Zhou,^{1,2} Wei Zhang,^{1,*} Jierong Cheng,¹ Yidong Huang,¹ and Jiande Peng¹

¹Department of Electronic Engineering, Tsinghua University Beijing, 100084, China

²betterchou@gmail.com

*Corresponding author: zwei@mail.tsinghua.edu.cn

Received May 26, 2009; revised August 12, 2009; accepted August 12, 2009;
posted August 17, 2009 (Doc. ID 111802); published September 4, 2009

Polarization-entangled photon pair generation based on two scalar scattering processes of the vector four-photon scattering has been demonstrated experimentally in high nonlinear microstructure fiber with birefringence. By controlling pump polarization state, polarization-entangled Bell states can be realized. It provides a simple way to realize efficient and compact fiber-based polarization-entangled photon pair sources.

© 2009 Optical Society of America

OCIS codes: 270.5585, 190.4380.

Polarization-entangled photon pair sources of $1.5 \mu\text{m}$ are important devices for quantum communication [1] and quantum information processing [2]. In recent years, spontaneous four-photon scattering (FPS) in optical fibers focuses much attention as a way to generate correlated/entangled photon pairs for its potential in realizing efficient and compact all-fiber $1.5 \mu\text{m}$ sources. To realize polarization entanglement in fibers, two schemes have been proposed, based on the time-multiplexing [3] and the polarization diversity loop [4].

Recently, high nonlinear microstructure fibers (HN-MSFs) have been looked at as important candidates for correlated/entangled photon pair generation. Compared with dispersion-shifted fibers in previous works, fiber length can be shortened to several meters [5,6] thanks to their high nonlinearity. Utilizing their unique dispersion characteristic, generation of correlated/entangled photon pairs can be extended to 800 nm band [6] and 800 nm/ $1.5 \mu\text{m}$ band [7,8].

On the other hand, nonignorable birefringence is an intrinsic characteristic of HN-MSFs [9]. Recently, vector FPS theory in fibers with birefringence [10] shows that two kinds of FPS processes take place simultaneously when pump light passes through birefringent fiber. One is the scalar scattering process, in which two annihilated pump photons and generated signal and idler photons are polarized along the same fiber polarization axis. The other is the vector scattering process, in which pump photons and signal and idler photons are polarized along two different fiber polarization axes. Frequencies of generated signal and idler photons through scalar and vector scattering processes are different, which provide feasibility to realize polarization-entangled photon pair generation directly in birefringent fibers.

In this Letter, we experimentally demonstrate that polarization-entangled photon pairs can be generated through the vector FPS in HN-MSFs with birefringence, and polarization-entangled Bell states can be realized by controlling pump-polarization state.

The experiment setup is shown in Fig. 1. The HN-MSF is 25 m long, fabricated by Crystal fiber A/S, Inc. (its scanning electron microscope image is shown in Fig. 1). The diameters of the silica core and air holes are $1.8 \mu\text{m}$ and $0.89 \mu\text{m}$, respectively. One of its zero-dispersion wavelengths is at 1564.8 nm . It has an ultrahigh nonlinear coefficient of 66.7 W/km , a phase birefringence of $\Delta n = 3.5 \times 10^{-5}$, and a group birefringence of $\Delta\beta_1 = 0.158 \text{ ps/m}$ at $1.5 \mu\text{m}$ [11,12].

The pulsed pump is generated by a passive mode-locked fiber laser, whose center wavelength, spectral width, and repeating frequency are 1552.75 nm , 0.2 nm and 1 MHz , respectively. A sideband suppression of 115 dB is realized by a filter system based on fiber Bragg gratings (FBGs), circulators (Cs), and tunable optical bandpass filters (TOBFs). The power and polarization state of pump are controlled by a variable optical attenuator (VOA1) and a polarizer (P), followed by a rotatable half-wavelength plate (HWP1) and a polarization controller (PC1), respectively. The generated correlated photon pairs are directed into two single-photon detectors (SPDs) through a filtering and splitting system based on FBGs, circulators, and TOBFs. Center wavelength and spectral width of selected signal photons are 1555.6 nm and 0.2 nm , respectively, while for idler ones 1549.9 nm and 0.2 nm . Total pump suppression

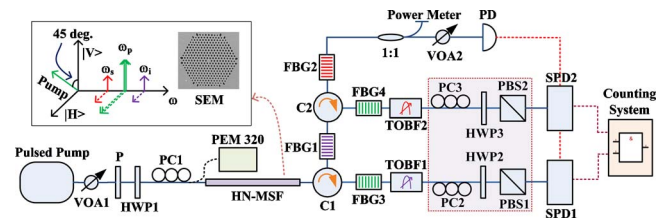


Fig. 1. (Color online) Experiment setup. VOA, variable optical attenuator; P, polarizer; HWP, half-wavelength plate; PC, polarization controller; C, circulator; FBG, fiber Bragg grating; TOBF, tunable optical bandpass filter; PBS, polarization beam splitter; PD, photon detector; SPD, single-photon detector.

is >105 dB for either signal or idler wavelengths. The two SPDs (Id201, Id Quantique) are operated in gated Geiger mode with a 2.5 ns detection window, triggered with residual pump light detected by a photon detector (PD).

The pump-polarization dependence property of correlated photon pair generation in the HN-MSF under a linearly polarized pump has been demonstrated [13]. It shows that the measured correlated photon pairs are generated by two independent scalar scattering processes in different fiber polarization axes, as shown in Fig. 1, and that the impact of polarization-dependent dispersion of the HN-MSF can be neglected in the experiment. Hence, polarization entanglement could be expected if pump polarization direction is not along the fiber axis, which can be realized by rotating HWP1 before the HN-MSF. When pump polarization direction is at 45° to fiber polarization axes, the generated polarization-entangled state has the form of $1/\sqrt{2}(|H_s\rangle|H_i\rangle + e^{i\varphi}|V_s\rangle|V_i\rangle)$, where H and V denote two fiber polarization axes, s and i denote the signal and idler photons, respectively, and φ is the relative phase difference between $|H_s\rangle|H_i\rangle$ and $|V_s\rangle|V_i\rangle$.

To demonstrate polarization entanglement of the generated photon pairs experimentally, two polarization analyzers are inserted before the two SPDs, shown in the dashed square in Fig. 1. Each polarization analyzer consists of a PC, a rotatable HWP, and a polarization beam splitter (PBS). First, the polarization direction of linearly polarized pump is set to the H axis. Hence generated correlated photon pairs and spontaneous Raman scattering (SpRS) photons are all polarized along the H axis. Adjusting PC2 to achieve maximum signal side count, the signal-side polarization analyzer can be collimated to the H axis. Rotating HWP2, the signal-side detecting direction (denoted by θ_s) can be rotated to any angle. Similarly, the idler-side detecting direction (denoted by θ_i) is collimated through PC3 and rotated by HWP3.

Then, polarization direction of the linearly polarized pump is adjusted to 45° to the H axis. Polarization-entangled characteristic of the generated photon pairs is demonstrated and shown in Fig. 2. Figure 2(a) is the coincidence count per 30 s (accidental coincidence count has been subtracted) under different θ_i . Squares and circles are the experiment data when θ_s is set to 135° and 0° , respectively. Solid and dashed curves are the fitting curves, showing that the fringe visibilities of two-photon interference are $96 \pm 3\%$ and $87 \pm 4\%$ for $\theta_s = 0^\circ$ and 135° , respectively.

Figure 2(b) is the idler-side photon count under different θ_i . Squares in the inset are measured results, which vary with θ_i owing to the generated SpRS photons copolarized with pump [14]. In the experiment, the pump level is low enough to ensure that the average number of generated photon per pulse is $\ll 1$ (typically 0.01 per pump pulse). Hence, the single side-counting rates of signal and idler photons (denoted by N_s and N_i , respectively) and the coincidence and accidental coincidence counting rates (de-

noted by N_{co} and N_{ac} , respectively) can be expressed as

$$N_s = \eta_s(R + R_s) + d_s,$$

$$N_i = \eta_i(R + R_i) + d_i,$$

$$N_{co} = \eta_s \eta_i (R + RR_s + RR_i + R_s R_i) + \eta_s (R + R_s) d_i + \eta_i (R + R_i) d_s,$$

$$N_{ac} = \eta_s \eta_i (R^2 + RR_s + RR_i + R_s R_i) + \eta_s (R + R_s) d_i + \eta_i (R + R_i) d_s, \quad (1)$$

where η_s and η_i are collection efficiencies of signal and idler photons and d_s and d_i are dark-count rates of SPDs at signal and idler sides ($\eta_s = 3.36\%$, $\eta_i = 2.38\%$, $d_s = 5.98 \times 10^{-5} \pm 1.001 \times 10^{-6}$, and $d_i = 4.67 \times 10^{-5} \pm 0.999 \times 10^{-6}$ measured during experiment setup preparation). R , R_s , and R_i are generation rates of the photon pairs and the SpRS photons at signal and idler wavelengths, respectively. The difference between N_{co} and N_{ac} in Eq. (1) is that they are coincidence counts of signal and idler photons generated from the same pump pulse and different pump pulses, respectively. We measure all N_s , N_i , N_{co} , and N_{ac} under each θ_i ($\theta_s = 0^\circ$ during the measurement) and calculate SpRS contribution to idler side photon count by solving Eq. (1). Dots in the inset of Fig. 2(b) are the calculated SpRS contribution, shown that it is main contribution of the idler side photon count variation. Main figure of Fig. 2(b) shows the contribution of generated photon pairs to idler side photon count. It does not vary with θ_i , demonstrating the polarization indistinguishable property at single side of the generated photon pair.

Figure 2 demonstrates that the generated photon pairs are in polarization-entangled state of $1/\sqrt{2}(|H_s\rangle|H_i\rangle + e^{i\varphi}|V_s\rangle|V_i\rangle)$ under a linearly polarized pump whose polarization direction is 45° to H axis. However, φ is unknown in the experiment, which limits its application as a polarization-entangled photon pair source. φ can be expressed as $\varphi = 2\varphi_p + \varphi_b$ in our experiment. φ_b is the fixed phase difference induced by fiber birefringence, and φ_p is phase difference determined by the initial pump-polarization state. Hence, φ can be controlled by adjusting the pump-polarization state. Especially, polarization-entangled Bell states $\Psi^\pm = 1/\sqrt{2}(|H_s\rangle|H_i\rangle \pm |V_s\rangle|V_i\rangle)$ can be realized while φ is $2n\pi$ and $2n\pi + \pi$ (n is an integer).

To control φ_p in this experiment, the pump is adjusted to be elliptically polarized by controlling PC1 and monitored by a polarization analyzer (Santec PEM-320) before it is injected into the HN-MSF. The long elliptical axis of pump is set to 45° to the H axis, while the power of pump light is unchanged. φ_p can be calculated by $\varphi_p = \pm \tan^{-1}(10^{-\text{PER}/10})$, where PER is the measured pump-polarization extinction ratio and $+$ and $-$ correspond to right- and left-handed elliptically polarized pump, respectively.

We measure the coincidence count (accidental coincidence count has been subtracted) under different

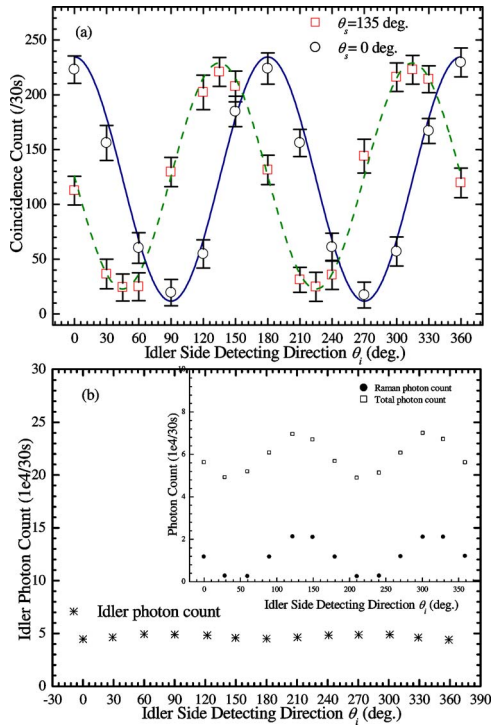


Fig. 2. (Color online) Experiment results of polarization entanglement demonstration: (a) coincidence count under different θ_i , (b) idler side photon count under different θ_i .

pump PERs when $\theta_s = 135^\circ$ and $\theta_i = 45^\circ$. The normalized coincidence count rate of the photon pairs, which is denoted by R_c , can be calculated by [3]

$$R_c = \sin^2 \theta_s \cos^2 \theta_i + \cos^2 \theta_s \sin^2 \theta_i + 2 \cos \varphi \sin \theta_s \cos \theta_s \sin \theta_i \cos \theta_i = 0.5[1 - \cos(2\varphi_p + \varphi_b)]. \quad (2)$$

By fitting the experiment data according to Eq. (2) and the relation between φ_p and PER, φ_b can be determined.

Figure 3 shows experiment results of polarization-entangled Bell states generation. The inset is the coincidence count under different pump PERs, while the solid curve is the fitting curve according to Eq. (2). It can be calculated that $\varphi_b = 0.23\pi$ in our experiment, and hence φ under each PER is determined. The main figure is the coincidence count plotted under different φ , which agrees well with Eq. (2). It can be seen that the maximum of the coincidence count indicates $\varphi = \pi$, leading to Ψ^- state, while the minimum indicates $\varphi = 0$, leading to Ψ^+ state. A theoretical two-photon interference visibility of 87.5% can be estimated under linearly polarized pump light, which agrees well with the experiment results in Fig. 2(a).

In summary, we demonstrate that based on two scalar scattering processes of the vector FPS in HN-

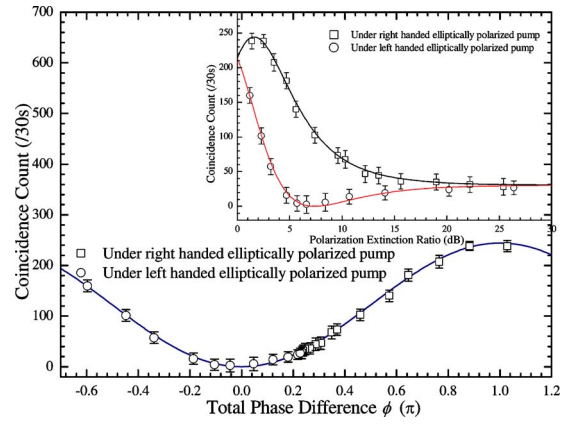


Fig. 3. (Color online) Polarization-entangled Bell states generation by controlling the pump-polarization state.

MSFs with birefringence, polarization-entangled photon pairs can be generated directly. Polarization-entangled Bell states can be realized by controlling the pump polarization state. It provides a simple way to realize efficient and compact fiber-based polarization-entangled photon pair sources.

This work was supported by National Natural Science Foundation of China (NSFC) under grant 60777032 and the National Basic Research Program of China (973) under grant 2010CB327600.

References

1. N. Gisin, G. Ribordy, W. Tittel, and H. Zbinden, *Rev. Mod. Phys.* **74**, 145 (2002).
2. C. H. Bennett and S. J. Wiesner, *Phys. Rev. Lett.* **69**, 2881 (1992).
3. X. Li, P. Voss, J. E. Sharping, J. Chen, and P. Kumar, *Phys. Rev. Lett.* **94**, 053601 (2005).
4. H. Takesue and K. Inoue, *Phys. Rev. A* **70**, 031802 (2004).
5. J. Fan, A. Migdall, and L. J. Wang, *Opt. Lett.* **30**, 3368 (2005).
6. J. Fulconis, O. Alibart, W. Wadsworth, P. Russell, and J. Rarity, *Opt. Express* **13**, 7572 (2005).
7. E. A. Goldschmidt, M. D. Eisaman, J. Fan, S. V. Polyakov, and A. Migdall, *Phys. Rev. A* **78**, 013844 (2008).
8. A. R. McMillan, J. Fulconis, M. Halder, C. Xiong, J. G. Rarity, and W. J. Wadsworth, *Opt. Express* **17**, 6156 (2009).
9. P. Russell, *J. Lightwave Technol.* **24**, 4729 (2006).
10. E. Brainis, *Phys. Rev. A* **79**, 023840 (2009).
11. Z. Wei, X. Li, Z. Lei, H. Yi-Dong, Y.-D. Huang, and J.-D. Peng, *Chin. Phys. Lett.* **23**, 1201 (2006).
12. X. Li, Z. Wei, Y.-D. Huang, and J.-D. Peng, *Chin. Phys. B* **17**, 995 (2008).
13. Q. Zhou, W. Zhang, S. Zhang, J. Cheng, Y. Huang, and J. Peng, *Optical Fiber Communications Conference* (Optical Society of America, 2009), paper OWD6.
14. Q. Lin, F. Yaman, and G. P. Agrawal, *Phys. Rev. A* **75**, 023803 (2007).